Supplementary Information

Dynamic single-molecule sensing via nanoparticle micromanipulation for rapid and ultrasensitive biomarker detection

Qiang Zeng[1#], Xiaoyan Zhou[1#], Yuting Yang[2#], Yi Sun[3], Jingan Wang[1], Chunhui Zhai[1], Jinghong Li[3*], Hui Yu[1,4*]

[1]School of Biomedical Engineering, Shanghai Jiao Tong University, Shanghai, 200030, People's Republic of China

[2]Department of Instrument Science and Engineering, School of Electronic Information and Electrical Engineering, Shanghai Jiao Tong University, Shanghai, 200030, People's Republic of China

[3]Department of Chemistry, Key Laboratory of Bioorganic Phosphorus Chemistry & Chemical Biology, Tsinghua University, Beijing, 100084, People's Republic of China

[4]Institute of Medical Robotics, Shanghai Jiao Tong University, Shanghai, 200030, People's Republic of China

[#]These authors contributed equally to this work.

[*]Correspondence should be addressed to: H.Y. (hui.yu@sjtu.edu.cn) or J.L. (jhli@mail.tsinghua.edu.cn)

Supplementary Note 1: Supporting Discussion

Typically, the clinical tests in an outpatient visit require less than 15 minutes assay time, and point-of-care testing may require even less. The assay time for single molecule sensors is largely limited by the mass transportation of fluorescence-labeled probes and the analyte onto the sensor surface. The diffusion rate in commonly used microfluidic channels could be estimated with typical values of less than 10 μm/s[1]. Considering a millimeter-order height of the channel, it takes at least minutes for the diffusion to complete, the diffusion rate was described by the Stocks-Einstein equation,

$$D_P = \frac{k_B T}{6\pi\eta r} \quad \text{(S1)},$$

Thus in typical experiments, the analyte needs to be incubated on the sensor surface for tens of minutes before detection.

Ideally, for dynamic sensing approaches such as the kinetic fingerprinting, they requires repetitive binding with a fast dissociation rate, but also a fast binding rate to reach equilibrium to shorten the assay time. However, simply changing the length of DNA probes or using low affinity antibodies could not satisfy both. For example, it has been reported that for a longer probe in the range of 6~9 nt, the binding rate (k_{on}) increased linearly, and the dissociation rate (k_{off}) decreased exponentially[2].

The SSM[3] circumvent the above limitations by the following designs. First, nanoparticles tethered high affinity probes are used to replace the fluorescence-labeled probes. The high affinity probes ensure a fast binding rate to capture analyte, and the nanoparticles are manipulated to actively transport the analyte to the sensor surface. This effectively breaks the limit by mass transportation. Second, to accelerate the dissociation during detection, an external force is applied on the nanoparticle as a load on the molecular complexes. As a result, the SSM[3] effectively shorten the assay time to within 15 minutes in the current system.

Supplementary Note 2: the limitation of endpoint ensemble measurement

In the endpoint ensemble measurement, it reports the total number of bound molecules at a specific time point τ, mostly after reaching equilibrium.

$$N(\tau) = \int_0^\tau (k_{\mathrm{on}}[\mathrm{A}]_t[\mathrm{P}]_t - k_{\mathrm{off}}[\mathrm{AP}]_t)\mathrm{d}t \ , \quad \text{(S2)}$$

The maximum readout is thus limited by the affinity of probes as

$$[\mathrm{AP}] = \frac{1}{K_d}[\mathrm{A}][\mathrm{P}] \quad \text{(S3)}$$

Supplementary Note 3: The surface coating density

The AuNPs are 50 nm in diameter and the tethered linker is ~ 25 nm for miRNA detection. The micro motion of AuNPs observed in the experiments is around 90 nm, which defines the maximum number of capture probes on planar sensor surface. Likewise, the linker for protein detection is ~ 120nm and the micro motion is about 130 nm. The surface density and coverage

area per analyte molecule are calculated as in Table S1.

Table S1. Molecular spacings of capture molecules on surfaces

	Surface density (molecules/μm^2)	Molecular spacing (nm)	Coverage area per molecule (nm^2/molecule)
miRNA capture probe	123	90	8156
$A\beta_{1\text{-}42}$ mAbs	59	130	16985

Supplementary Note 4: ROC plot, and discrimination factor Q calculation

The specificity of an assay is calculated from the number of true negatives (TN) and false positives (FP) according to the relationship:

$$specificity = \frac{TN}{TN+FP} \quad \text{(S4)}$$

The discrimination factor Q was calculated as:

$$Q = \frac{Events\ of\ target\ analyte}{Events\ \ of\ undesired\ molecule} \quad \text{(S5)}$$

Supplementary Note 5: Size and zeta potential of NPs

Table S2. Molecular spacings of capture molecules on surfaces.

Type of detection probe	Size (nm)	Zeta potential (mV)
ssDNA-GNP	74.8±0.07	-31.67±1.38
mAb-GNP	68.1±1.24	-27.16±2.48

Supplementary Note 6: miRNA synthesis and probe design.

For miRNA detection experiments, the corresponding sequences were shown in **Table S3.** Note that the red-marked capture probe sequences represent lock nucleic acid (LNA) rather than DNA nucleotides, which provide much higher affinity to the target analyte. The capture probe was thiol-functionalized at 3' and both detection probes were biotin-functionalized at 5'.

Table S3. The miRNAs and corresponding capture probes and detection probes.

Name		Sequence		length
miR-21	5'	UAGCUUAUCA GACUGAUGUUGA	3'	22 nt
Capture probe	3'	HS- ATCGAATAGT	5'	10 nt
Detection probe	3'	CTGACTACAACT -biotin	5'	12 nt
miR-155	5'	UUAAUGCUAAU CGUGAUAGGGGU	3'	23 nt
Capture probe	3'	HS- AATTACGATTA	5'	11 nt
Detection probe	3'	GCACTAT CCCCA -biotin	5'	12 nt
miR-362	5'	AAUCCUUGGAAC CUAGGUGUGAGU	3'	24 nt

Capture probe	3’	HS-TTAGGAACCTTG		5’	12 nt
Detection probe	3’		GATCCACACTCA -biotin	5’	12 nt

For single base pair mismatch experiments, the sequences are listed in the **Table S4**. The detection probe was designed to be complementary to *miR-29a* but with one base pair mismatch to *miR-29c*.

Table S4. The miRNAs and oligonucleotides probes for single base pair mismatch experiments.

Name		Sequence		length
miR-29a	5’	UAGCACCAUCUG AAAUCGGUUA	3’	22 nt
miR-29c	5’	UAGCACCAUUUG AAAUCGGUUA	3’	22 nt
Detection probe	3’	biotin- ATCGTGGTAGAC	5’	12 nt
Capture probe	3’	TTTAGCCAAT -SH	5’	10 nt

References

1. Squires TM, Messinger RJ, Manalis SR. Making it stick: convection, reaction and diffusion in surface-based biosensors. *Nat Biotechnol* 2008, **26**(4)**:** 417-426.
2. Dupuis NF, Holmstrom ED, Nesbitt DJ. Single-molecule kinetics reveal cation-promoted DNA duplex formation through ordering of single-stranded helices. *Biophys J* 2013, **105**(3)**:** 756-766.

Figure S1 Typical bound lifetime profiles.

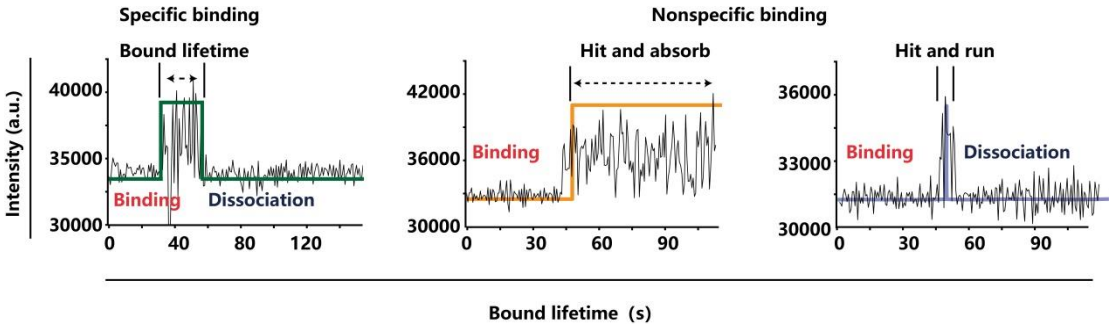

Figure S2 Bound lifetime distribution of three miRNA (a, b and c) and control group without analyte (d). The bound time was determined via exponential fitting, the values were **22.94 ± 7.49s** for *has-miR-21*, **27.26 ± 8.93s** for *has-miR-155*, **12.67 ± 2.35s** for *has-miR-362* and **4.11 ± 0.26s** for control, respectively.

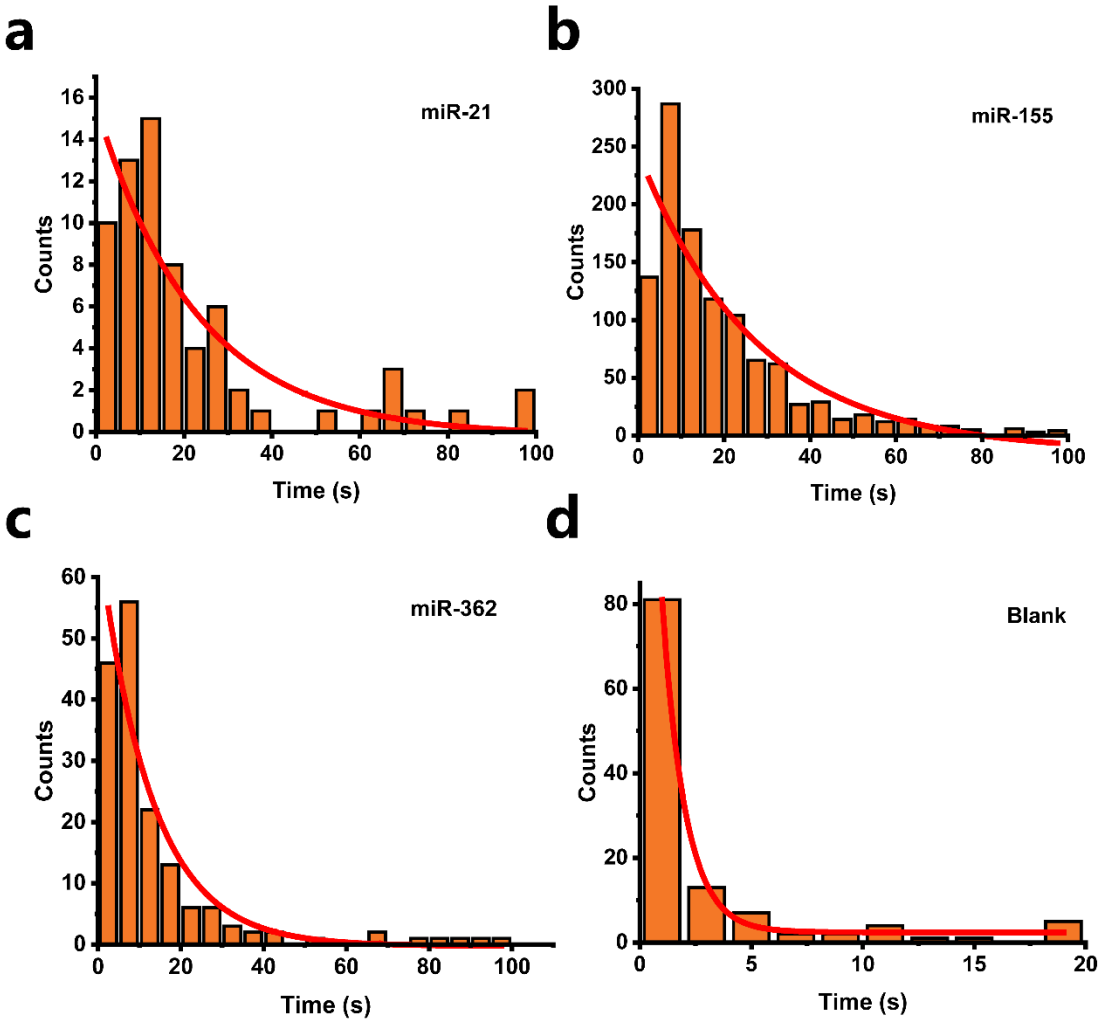

Figure S3 Time-dependent coefficient of variation (CV) in the number of AuNPs association and dissociation events. The CV is calculated by standard deviations divide by the average, which scales with 1/ √ N (N is the number of events). The CV for low concentration analyte decreased below 15% until **13.5** min. We thus conclude that 15-min assay is sufficient.

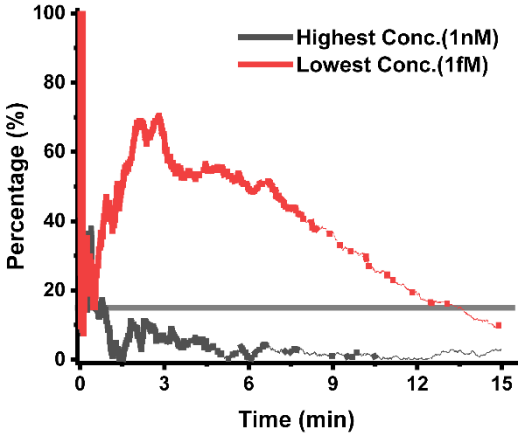

Figure S4 The ROC plot of *has-miR-29a* detection with (blue line), or without (red line) the presence of *has-miR-29c*. The AUC values are **0.816 and 0.979** respectively.